



**HAL**  
open science

## Highly para-selective alkylation of toluene by methyl mercaptan over silylated ZSM-5 zeolite

Abdelilah Bayout, Claudia Cammarano, Izabel Medeiros Costa, Gleb Veryasov, Alexander Sachse, Vasile Hulea

► **To cite this version:**

Abdelilah Bayout, Claudia Cammarano, Izabel Medeiros Costa, Gleb Veryasov, Alexander Sachse, et al.. Highly para-selective alkylation of toluene by methyl mercaptan over silylated ZSM-5 zeolite. Journal of Catalysis, 2024, 440, pp.115828. 10.1016/j.jcat.2024.115828 . hal-04778093

**HAL Id: hal-04778093**

**<https://hal.science/hal-04778093v1>**

Submitted on 12 Nov 2024

**HAL** is a multi-disciplinary open access archive for the deposit and dissemination of scientific research documents, whether they are published or not. The documents may come from teaching and research institutions in France or abroad, or from public or private research centers.

L'archive ouverte pluridisciplinaire **HAL**, est destinée au dépôt et à la diffusion de documents scientifiques de niveau recherche, publiés ou non, émanant des établissements d'enseignement et de recherche français ou étrangers, des laboratoires publics ou privés.

# Highly *para*-selective alkylation of toluene by methyl mercaptan over silylated ZSM-5 zeolite

Abdelilah Bayout<sup>a</sup>, Claudia Cammarano<sup>a</sup>, Izabel Medeiros Costa<sup>b</sup>, Gleb Veryasov<sup>c</sup>, Alexander Sachse<sup>d</sup>, Vasile Hulea<sup>a,\*</sup>

<sup>a</sup> Charles Gerhardt Institute of Montpellier, University of Montpellier, CNRS, ENSCM, 1919 Rte de Mende, 34293 Montpellier Cedex 5, France

<sup>b</sup> TotalEnergies One Tech, Courbevoie, France

<sup>c</sup> Total Energies One Tech, Zone Industrielle C, 7181, Feluy, Belgium

<sup>d</sup> Institut de Chimie des Milieux et Matériaux de Poitiers (IC2MP) - UMR 7285 CNRS, UFR SFA, Université de Poitiers, Bât. B27, 4 rue Michel Brunet, TSA 51106, Poitiers 86073 Cedex 9, France

## ARTICLE INFO

### Keywords:

Methyl mercaptan  
Toluene  
Para-xylene  
Alkylation  
ZSM-5 zeolite  
Silylation

## ABSTRACT

Friedel-Crafts alkylation of toluene with methyl mercaptan has been investigated in the presence of H-ZSM-5 and SiO<sub>2</sub>/H-ZSM-5 catalysts. The silica layers have been built on H-ZSM-5 zeolite by chemical liquid deposition of tetraethyl orthosilicate. The passivation with silica of the external surface of H-ZSM-5 zeolite has been confirmed by FT-IR spectroscopy and mesitylene isomerization, used as a model reaction. All catalysts exhibited notable behavior in the alkylation of toluene to xylenes. Efficiencies higher than 98 % in alkylation for both toluene and methyl mercaptan were obtained at 375 °C. In terms of *para*-selectivity, outstanding performance was revealed by the silylated zeolites. Thus, over 12 % SiO<sub>2</sub>/H-ZSM-5, at 375 °C and WHSV = 9.4 g<sub>toluene</sub>-CH<sub>3</sub>SH g<sub>cat</sub><sup>-1</sup>h<sup>-1</sup>, the *para*-xylene selectivity was close to 100 %. The experimental apparent activation energy for the toluene alkylation with methyl mercaptan catalyzed by H-ZSM-5 was 80 kJ/mol.

## 1. Introduction

In a recent study [1] it has been shown that the reaction between toluene and methyl mercaptan catalyzed by zeolites follows a Friedel-Crafts mechanism to produce a mixture of aromatics, dominated by xylenes. The encouraging results obtained recommend this reaction as a promising route for the simultaneous valorization of both toluene (a low-cost feedstock, which is in excess on the market) and CH<sub>3</sub>SH (an abundant contaminant in natural gas).

In order to gather more knowledge on this alkylation process, we extended the research over ZSM-5 type catalysts. First, kinetic parameters, such as rate constants and activation energy, were calculated and compared with those previously obtained for the toluene alkylation with methanol. Afterward, we prepared and characterized ZSM-5 based catalysts able to produce selectively *para*-xylene from toluene and methyl mercaptan. In existing commercial applications, *para*-xylene accounts for more than 85 % of total xylenes. With an annual global demand of more than 60 million tons, *para*-xylene is among the most important intermediates used in the production of polymers and organic chemicals [2]. Basically, it is produced, along with meta- and *ortho*-xylene, from

catalytic reforming and steam cracking of naphtha [3]. Alternative methods, such as toluene disproportionation and toluene-trimethylbenzene transalkylation are also commercialized in refineries in order to ensure the market demand for xylenes.

A particular method, which allows to obtain more selectively *para*-xylene, is the acid catalyzed alkylation of toluene by methanol. Exhaustive industrial and academic research made on this subject showed that the medium-pore acidic zeolites, and in particular ZSM-5 zeolite, were the most performant catalysts for this reaction [4–7]. Unfortunately, the efficiency of methanol in alkylation is not satisfactory for large industrial applications.

The *para*-selectivity is usually ascribed to diffusional properties of these zeolites. Indeed, it was shown that the intracrystalline diffusion rate of *para*-xylene is considerably higher than that of the bulkier *ortho*- and *meta*-xylene [8,9]. Moreover, this difference can be enhanced by tailoring the pore openings and the size/morphology of the zeolite crystals [10,11]. Nevertheless, once out of the zeolite pores, due to the presence of the acid sites on the external surface, *para*-xylene easily isomerizes to its isomers. The passivation of the external surface by impregnation with various chemical species, including SiO<sub>2</sub> [12–14],

\* Corresponding author.

E-mail address: [vasile.hulea@enscm.fr](mailto:vasile.hulea@enscm.fr) (V. Hulea).

P<sub>2</sub>O<sub>5</sub> and B<sub>2</sub>O<sub>3</sub> [15], MgO [16] and ZnO [17] proved to be a very effective way to avoid *para*-xylene isomerization. Thus, *para*-selectivities over 90 % have been frequently reported with these catalysts.

By analogy with the reaction between toluene and methanol, we studied here the reaction between toluene and methyl mercaptan using a series of SiO<sub>2</sub>/ZSM-5 catalysts. ZSM-5 zeolite (Si/Al = 15) was modified by coating its surface with a SiO<sub>2</sub> layer generated by chemical liquid deposition of tetraethyl orthosilicate. The catalytic behavior and particularly the high *para*-selectivity have been related to the amount of SiO<sub>2</sub> and the reaction conditions.

## 2. Experimental

### 2.1. Materials and catalysts

Zeolite ZSM-5 (Si/Al = 15) was purchased from Zeolyst International. The surface modified-H-ZSM-5 were prepared as follows: 1 g of zeolite was dispersed in 25 mL of hexane (>99 %, Sigma-Aldrich), then 144.2 mg of tetraethyl orthosilicate (TEOS, >99 %, Sigma-Aldrich) was added (representing 4 % SiO<sub>2</sub> per gram of zeolite). The mixture was heated to 80 °C for 1 h under stirring at 250 rpm. After hexane removal by evaporation, the resulting solid was dried at 80 °C for 16 h, then calcined in a muffle furnace at 550 °C at 5 °C/min for 8 h to obtain the zeolite H-ZSM-5 modified with 4 % SiO<sub>2</sub>. This procedure was repeated two or three times to obtain three modified-HZSM-5 with different loading amounts of SiO<sub>2</sub> (4 %, 8 % and 12 % by weight of SiO<sub>2</sub>). The resulting samples were denoted as 4 %SiO<sub>2</sub>/H-ZSM-5, 8 %SiO<sub>2</sub>/H-ZSM-5, 12 %SiO<sub>2</sub>/H-ZSM-5.

### 2.2. Catalyst characterization

The crystallinity of the catalysts was examined by X-ray diffraction, in the range  $2\theta = 4 - 50^\circ$  with an angular step size of  $0.0197^\circ$  and an acquisition time of 0.2 s (Bruker D8 Advance device with a Bragg-Brentano configuration, Bruker Lynx Eye detector, Cu K $\alpha$  radiation). Nitrogen physisorption measurements were carried out at  $-196^\circ\text{C}$  on a Micromeritics Tristar sorptomer, using samples outgassed under vacuum at  $250^\circ\text{C}$  for 6 h. The specific surface area was determined by using the BET technique. The micropore area and volume and the external surface area were determined by using the t-plot method.

The temperature-programmed desorption of ammonia (NH<sub>3</sub>-TPD) was used for evaluating the acidity of the H<sup>+</sup>-form zeolites. Before NH<sub>3</sub> adsorption, 50 mg of zeolite was treated under an air flow ( $30\text{ mL min}^{-1}$ ) at  $550^\circ\text{C}$  at  $10^\circ\text{C min}^{-1}$  for 2 h, in a Micromeritics Autochem II apparatus. The pretreated sample was then equilibrated in an ammonia stream (5 % NH<sub>3</sub> in He,  $45\text{ mL min}^{-1}$ ) at  $100^\circ\text{C}$  for 40 min, followed by a purge in helium at the same temperature, until the baseline of the TC detector was stable. Ammonia desorption was carried out under a helium flow ( $25\text{ mL min}^{-1}$ ) at  $10^\circ\text{C min}^{-1}$  up to  $600^\circ\text{C}$ . A TCD signal calibration allowed to quantify the acidity of solids.

**Table 1**  
Main properties of the catalysts.

	H-ZSM-5	4 %SiO <sub>2</sub> / H-ZSM-5	8 %SiO <sub>2</sub> / H-ZSM-5	12 %SiO <sub>2</sub> / H-ZSM-5
SiO <sub>2</sub> , wt%/Total surface area	–	4	8	12
(BET) <sup>a</sup> , m <sup>2</sup> g <sup>-1</sup> External surface area	412	400	390	370
(BET) <sup>b</sup> , m <sup>2</sup> g <sup>-1</sup> Micropore surface area	63	15	5	3
(BET) <sup>b</sup> , m <sup>2</sup> g <sup>-1</sup>	475	415	395	373
Micropore volume <sup>b</sup> , mL g <sup>-1</sup>	0.176	0.164	0.159	0.150
Total acidity <sup>c</sup> , $\mu\text{mol}_{\text{NH}_3} \text{g}_{\text{cat}}^{-1}$	790	710	620	490
Weak acidity <sup>d</sup> , $\mu\text{mol}_{\text{NH}_3} \text{g}_{\text{cat}}^{-1}$	460	430	390	310
Strong acidity <sup>d</sup> , $\mu\text{mol}_{\text{NH}_3} \text{g}_{\text{cat}}^{-1}$	340	280	230	180

<sup>a</sup> Surface area determined from nitrogen isotherms, using the BET method.

<sup>b</sup> Calculated using the t-plot method.

<sup>c</sup> Total amount of acid sites, determined from the ammonia TPD experiments.

<sup>d</sup> Determined by the deconvolution of the TPD profiles.

FTIR spectra were recorded before and after pyridine adsorption on a Nicolet 5700 instrument. The material was first compressed (0.5 T) to form a self-supported pellet (2 cm<sup>2</sup>, 10–30 mg) and heated at  $450^\circ\text{C}$  under air flow ( $60\text{ mL min}^{-1}$ ). The sample was then outgassed ( $10^{-5}$  bar) at  $200^\circ\text{C}$  for 1 h before to register the first FTIR spectrum. The sample was cooled to RT and exposed to pyridine (1.5 mbar) for 5 min and outgassed ( $10^{-5}$  bar) to remove physisorbed pyridine at  $150^\circ\text{C}$ . The quantification of Brønsted and Lewis acid sites was realized by integration of the bands at 1545 and  $1455\text{ cm}^{-1}$ , respectively, using the following extinction coefficients:  $\epsilon_{1545} = 1.13$  and  $\epsilon_{1455} = 1.28\text{ cm}^2 \mu\text{mol}^{-1}$ .

The catalysts used in reactions were characterized by thermal gravimetric-mass spectrometry analysis (TGA-MS). Before characterization, after the reaction run, the reactor was flushed with nitrogen at  $375^\circ\text{C}$  for 30 min, in order to desorb the volatile species confined in the catalyst. The TGA-MS measurements were performed on a STA 449 F1 Jupiter instrument coupled to a mass spectrometer QMS 403 Aeolos Quadro. 10 mg of spent catalyst were heated from 40 to  $800^\circ\text{C}$  at  $10^\circ\text{C min}^{-1}$  in an air flow ( $30\text{ mL min}^{-1}$ ).

### 2.3. Catalytic testing

The catalytic alkylation of toluene with methyl mercaptan was performed under atmospheric pressure, in continuous mode, using a stainless-steel plug flow reactor (0.45 cm ID, L = 13.6 cm). Prior to the reaction, the catalyst (30 mg, 150–250  $\mu\text{m}$  particle size, mixed with 120 mg of quartz) was activated at  $550^\circ\text{C}$  for 8 h (heating rate of  $5^\circ\text{C min}^{-1}$ ) in an airflow. Then, under a nitrogen flow ( $30\text{ mL min}^{-1}$ ), the catalyst was brought to the reaction temperature. In a typical run, a premixed feed consisting of toluene/CH<sub>3</sub>SH/nitrogen = 2.5/2.5/95 (mol/mol/mol) was introduced into the reactor with a total flow rate of  $30\text{ mL min}^{-1}$ . The complete reactor effluent was analyzed online by gas chromatography, using two apparatus/columns/detectors. The hydrocarbons were analyzed on a Varian 3900, CP-WAX-57-CB (25 m x 0.32 mm x 0.20  $\mu\text{m}$ ), FID, while the S-containing compounds were analyzed on a Shimadzu GC 2014, Supel-Q Plot (30 m x 0.32 mm x 0.15  $\mu\text{m}$ ), FPD.

The mesitylene (1,3,5-Trimethylbenzene) conversion in isomerization was used such as probe reactions to evaluate the external surface acidity of parent and modified H-ZSM-5. This reaction was carried out in the fixed-bed reactor at  $375^\circ\text{C}$  and atmospheric pressure with 30 mg of catalyst, and WHSV =  $3.54\text{ h}^{-1}$ . The reaction products were analyzed online by gas chromatography on a Varian 3900, CP-WAX-57-CB (25 m x 0.32 mm x 0.20  $\mu\text{m}$ ), FID.

## 3. Results and discussion

### 3.1. Catalyst characteristics

The X-ray diffraction patterns reported in Fig. S1 (Supplementary Material) confirmed that the samples modified with silica conserved the

crystallinity of the parent zeolite. The nitrogen adsorption isotherms (at  $-196\text{ }^{\circ}\text{C}$ , Fig. S2) are typical of microporous materials and show that the total pore volumes of the silylated samples are lower than that of the unmodified zeolite and gradually decrease with increasing the  $\text{SiO}_2$  content. This suggests that the silylation process removed most of the inter-crystalline porosity present in the parent zeolite. *t*-Plot analysis was used to accurately determine the textural characteristics of the catalysts (Fig. S3). The results compiled in Table 1 show that the external surface greatly decreases after silica deposition. Also, the internal surface and micropore volumes decrease after silylation. This is an indication that the silylation preferentially occurred on the external surface and in the pore mouth region, as previously established by the Lercher group [18].

The acidity of the catalysts was evaluated by ammonia TPD. The parent and the silylated samples exhibited typical  $\text{NH}_3$ -TPD profiles, with two peaks at about  $200\text{ }^{\circ}\text{C}$  and  $425\text{ }^{\circ}\text{C}$ , representing respectively the ammonia desorbed from weak and strong acid sites (Fig. S4).

For the silylated catalysts, a gradual decrease in the intensity of both desorption peaks with increasing  $\text{SiO}_2$  content was observed. The concentrations of the acid sites are summarized in Table 1. It is important to note that the ratio between the weak and strong acid sites slightly increased with increasing the amount of silica in the catalyst (Table 1, Fig. S5).

The acidity of the catalysts was further evaluated by FT-IR spectroscopy. The IR spectra recorded in the region of hydroxyl functions before adsorption of the pyridine are compared in Fig. 1. Two distinct bands changed in intensity after silylation. The first centered at  $3745\text{ cm}^{-1}$  (which correspond to the terminal silanol groups located mainly on the external surface) significantly decreased for both 4 % $\text{SiO}_2$ /H-ZSM-5 and 12 % $\text{SiO}_2$ /H-ZSM-5. Similarly, the band at  $3608\text{ cm}^{-1}$  (attributed to the Brønsted acid sites) suffered severe reduction in intensity after modification with silica.

Fig. 2a and 2b compare the IR spectra recorded before and after pyridine adsorption for ZSM-5 and 12 % $\text{SiO}_2$ /H-ZSM-5, respectively. For both samples, the band at  $3608\text{ cm}^{-1}$  almost completely disappeared after pyridine adsorption, indicating that the acidic sites are fully accessible for pyridine. Similarly, the band at  $3660\text{ cm}^{-1}$  (assigned to the hydroxyls associated with the EF-Al species located at the internal surface) strongly decreased after pyridine adsorption.

The IR spectra after pyridine adsorption in the region of  $1440\text{--}1700\text{ cm}^{-1}$  are displayed in Fig. 3. The bands at  $1545\text{ cm}^{-1}$  (attributed to pyridinium ions formed by Brønsted acid sites) and  $1454\text{ cm}^{-1}$  (attributed to pyridine molecules coordinated on Lewis acid sites) were quantitatively evaluated and the values are compiled in Table 2.

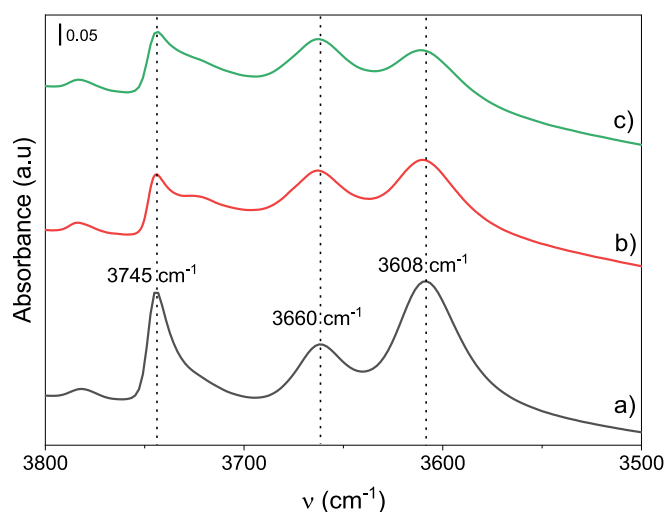


Fig. 1. IR spectra in the region of hydroxyl group vibrations (before adsorption of the pyridine); a) H-ZSM-5, b) 4% $\text{SiO}_2$ /H-ZSM-5, c) 12% $\text{SiO}_2$ /H-ZSM-5.

These results show a noticeable loss in the number of the Brønsted acid sites for the silylated samples. The loss is comparative to the quantity of silica deposited over ZSM-5 zeolite. In contrast, the number of the Lewis acid sites slightly increased.

The passivation of the external surface of zeolites after silylation was additionally examined by performing the isomerization of mesitylene (1,3,5-trimethylbenzene, TMB) as a model reaction. Note that mesitylene has a molecular size too large to penetrate the channels of the H-ZSM-5 zeolite [19] hence its conversion is merely ensured by the external acid sites. Only the isomerization of the mesitylene into 1,2,4-TMB and 1,2,3-TMB occurred under our experimental conditions (Fig. S6). In the presence of the unmodified zeolite, the total conversion of the 1,3,5-TMB was 52 %. In contrast, over the 12 % $\text{SiO}_2$ /HZSM-5 catalyst, only 4 % of the reagent was involved in the isomerization reaction (Table 3).

These results clearly prove that the silylation process invalidated most of the external Brønsted acid sites contained in the parent zeolite. As previously stated, the deactivation of the Brønsted acid sites is due to their reaction (hydrolysis) with TEOS [18]. As the diameter of TEOS is larger than of the pores of MFI zeolite, silylation occurred mainly on the external surface.

### 3.2. Toluene alkylation with methyl mercaptan – Catalytic behavior

#### 3.2.1. General aspect

In the previous publication [1] we studied the alkylation of toluene by methyl mercaptan over zeolites with different topologies. The catalytic runs, carried out at  $375\text{ }^{\circ}\text{C}$ , during 6.5 h on stream, revealed that H-ZSM-5 was the most performant catalyst in terms of both alkylation yield and deactivation stability.

At the beginning of the present study, we examined the behavior of this zeolite in a longer-term experiment. The experimental data showed that during 36 h on stream, the conversion of toluene (27 %) and methyl mercaptan (60 %) did not vary (Fig. S7). The main hydrocarbons in process included para-, meta- and ortho-xylenes and trimethylbenzenes (Fig. S8a). Traces of C1-C3 hydrocarbons, benzene and tetramethylbenzenes were also produced. Dimethyl sulfide and hydrogen sulfide were the only S-containing molecules obtained in the process (S8b). These molecules result either from  $\text{CH}_3\text{SH}$ , by a zeolite-catalysed condensation reaction ( $2\text{CH}_3\text{SH} \rightarrow \text{CH}_3\text{SCH}_3 + \text{H}_2\text{S}$ ) [1], or from toluene alkylation ( $\text{C}_6\text{H}_5(\text{CH}_3) + \text{CH}_3\text{SH} \rightarrow \text{C}_6\text{H}_4(\text{CH}_3)_2 + \text{H}_2\text{S}$ ).

The ratio between xylenes and trimethylbenzenes was 70:30 and that between para-, meta- and ortho-xylenes was 37:47:16. These ratios did not fluctuate during the catalytic run (Fig. S9).

In Scheme 1 are included the reactions explaining the formation of the products identified in the process. Note that these reactions are similar to those usually observed in the toluene alkylation by methanol over zeolites [20].

The experimental data showed that more than 99 % of toluene converted was involved in alkylation, to produce xylenes and trimethylbenzenes. On the other hand, the methyl mercaptan was consumed in three reactions. A significant part was transformed into dimethyl sulfide, a part was involved in the alkylation (to produce xylenes and trimethylbenzenes) and a small amount was transformed into light aliphatic hydrocarbons. If we treat methyl mercaptan and dimethyl sulfide as a single alkylating agent (because dimethyl sulfide is also an alkylating agent, as showed in ref. [1]), we can state that the fraction of the methyl mercaptan involved in the toluene alkylation (called alkylation efficiency) was about 98 %.

It should be noted that this value is superior to most of those reported in literature for the toluene alkylation with methanol in the presence of zeolites, under comparable process parameters [20]. To confirm, we carried out an experiment using the methanol as methylating agent for toluene, under conditions identical to those described above (H-ZSM-5,  $m_{\text{cat}} = 30\text{ mg}$ ,  $T = 375\text{ }^{\circ}\text{C}$ , volume flow rate =  $30\text{ mL min}^{-1}$ ; toluene/ $\text{CH}_3\text{OH} = 1/1$ ,  $\text{WHSV} = 8.3\text{ g}_{\text{toluene}+\text{CH}_3\text{OH}}\text{ g}_{\text{cat}}^{-1}\text{h}^{-1}$ ). The toluene

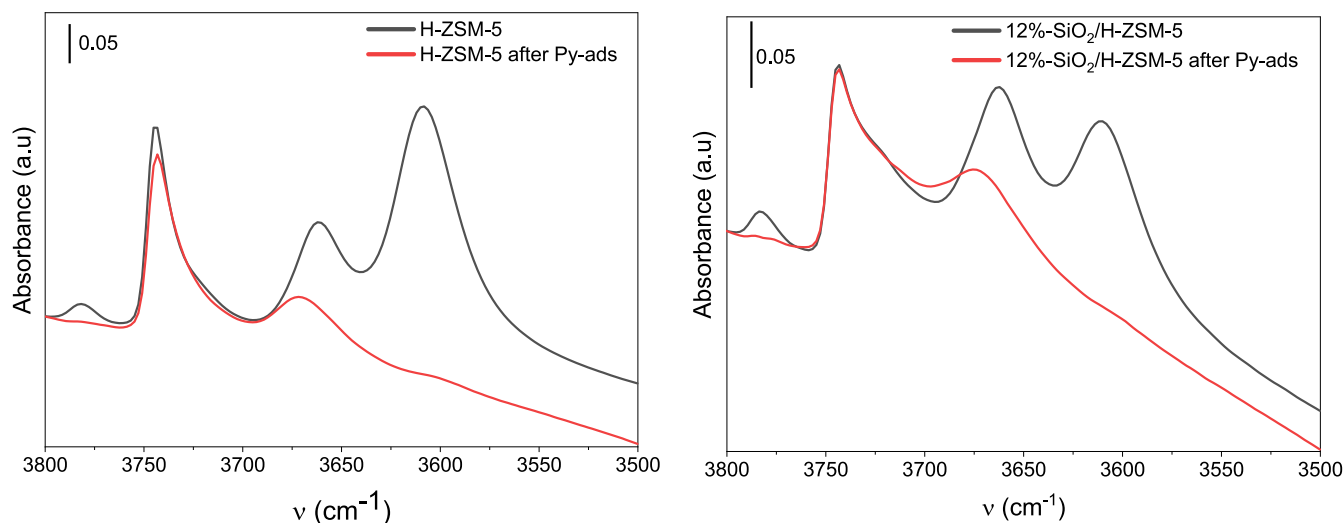


Fig. 2. a. IR spectra in the region of hydroxyl group vibrations (before and after adsorption of the pyridine) for H-ZSM-5. Fig. 2b. IR spectra in the region of hydroxyl group vibrations (before and after adsorption of the pyridine) for 12%SiO<sub>2</sub>/H-ZSM-5.

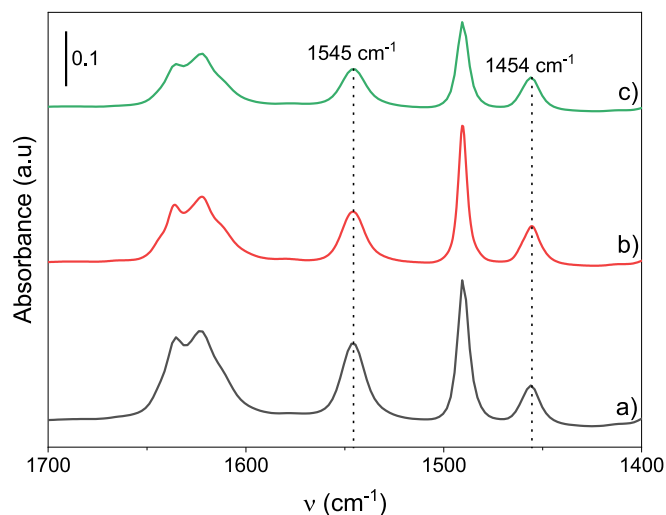


Fig. 3. IR spectra of activated a) H-ZSM-5, b) 4 %SiO<sub>2</sub>/H-ZSM-5 and c) 12 % SiO<sub>2</sub>/H-ZSM-5 (after adsorption of pyridine and evacuation at 150 °C).

**Table 2**  
Concentration of Brønsted and Lewis acid sites determined by adsorption of pyridine (μmol/g).

Catalyst	Brønsted acid sites		Lewis acid sites		Total	
	150 °C <sup>a</sup>	350 °C <sup>a</sup>	150 °C	350 °C	150 °C	350 °C
H-ZSM-5	470	310	110	75	580	385
4 %SiO <sub>2</sub> /H-ZSM-5	340	245	160	90	500	335
ZSM-5	(354) <sup>b</sup>	(255)	(170)	(95)	(524)	(350)
12 %SiO <sub>2</sub> /H-ZSM-5	250	135	130	65	380	200
H-ZSM-5	(284)	(155)	(148)	(75)	(432)	(230)

<sup>a</sup> Evacuation temperature after pyridine adsorption

<sup>b</sup> In brackets are the values normalized to the weight of the zeolite in the catalyst.

conversion was 28 %, the overall methanol conversion was 100 % and the methanol conversion in alkylation was 33 %. About 65 % of methanol was involved in the formation of C1-C6 aliphatic hydrocarbons (Fig. S10).

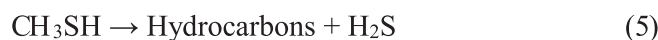
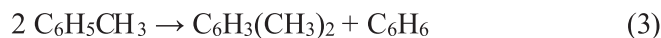
### 3.2.2. Kinetic study over H-ZSM-5 catalyst

For the reactions carried out in flow, the weight hourly space

**Table 3**  
Mesitylene isomerization.<sup>a</sup>

Catalyst	Mesitylene conversion, %	Products, %	
		1,2,4-TMB	1,2,3-TMB
H-ZSM-5	52	55	12
12 %SiO <sub>2</sub> /H-ZSM-5	4	> 99	< 1

<sup>a</sup> Conditions: T = 375 °C, catalyst mass = 30 mg, gas flow rate = 30 mL min<sup>-1</sup>.



**Scheme 1.** Reactions involved in the process: (1) toluene alkylation, (2) xylenes alkylation, (3) toluene disproportionation, (4) methyl mercaptan conversion into dimethyl sulfide, (5) methyl mercaptan conversion into hydrocarbons.

**Table 4**  
Toluene conversion (%) at various temperatures and WHSV.

T (°C)	WHSV (g <sub>toluene</sub> g <sub>cat</sub> <sup>-1</sup> h <sup>-1</sup> )		
	6.2	3.1	2.0
375	26.1	42.4	55.9
400	40.5	58.3	73.6
425	55.1	76.4	88.5

velocity (WHSV) calculated from the reactants mass flow and the catalyst mass is a crucial parameter. We examined the effect of this parameter on the alkylation reaction conducted at various temperatures, using 30, 60 et 90 mg of zeolite ZSM-5. This corresponds to a WHSV of 6.2, 3.1 and 2.0 g<sub>toluene</sub> g<sub>cat</sub><sup>-1</sup> h<sup>-1</sup>, respectively. As expected, when the weight hourly space velocity decreased from 6.2 to 2.0 h<sup>-1</sup>, the toluene conversion significantly increased (Table 4).

Data summarized in Table 4 allowed us to quantify some kinetic parameters, such as rate constants and activation energy, and to



compare these values to previous studies investigating the toluene alkylation with methanol. Most of the kinetic studies developed for the alkylation of toluene with methanol or dimethyl ether on zeolites have shown a first-order dependence on toluene and a zero-order dependence on the methylating agent [21–24]. This behavior is due to the fact that the acid sites of the catalyst are easily covered with methoxy-species, which react with toluene in the rate-determining step. By analogy, we treated the present results considering a first-order kinetic for toluene and zero-order for methyl mercaptan. The rate constants obtained at various temperatures are given in Table 5.

The apparent activation energy, obtained from Arrhenius plots, was  $80 \text{ kJ mol}^{-1}$ . This value is larger compared to the activation energies reported for the toluene methylation over ZSM-5 catalysts, which varied between 50 and  $60 \text{ kJ mol}^{-1}$  [22–24].

### 3.2.3. Para-selective alkylation over $\text{SiO}_2/\text{ZSM-5}$ catalysts

In this section we examined the catalytic properties of 4 % $\text{SiO}_2/\text{H-ZSM-5}$ , 8 % $\text{SiO}_2/\text{H-ZSM-5}$  and 12 % $\text{SiO}_2/\text{H-ZSM-5}$  samples. The catalytic experiments were carried out under the following conditions:  $m_{\text{cat}} = 30 \text{ mg}$ ,  $T = 375 \text{ }^\circ\text{C}$ , flow rate =  $30 \text{ mL min}^{-1}$ , toluene/ $\text{CH}_3\text{SH} = 1/1$ ,  $\text{WHSV} = 9.4 \text{ g}_{\text{toluene}+\text{CH}_3\text{SH}} \text{ g}_{\text{cat}}^{-1} \text{ h}^{-1}$ .

Usually, the reactions catalyzed by zeolites mainly occur in the micropores of the catalysts. In the case of H-ZSM-5, toluene and methyl mercaptan, as well as the low aromatic products may easily diffuse through the pores. As a result, the reactions involving these reagents are not prevented (Fig. S8a and S8b). In the case of  $\text{SiO}_2/\text{ZSM-5}$  samples, the diffusion of the aromatic molecules can be restricted in the narrowed pores, while the diffusion of the small  $\text{CH}_3\text{SH}$  molecules is less limited in these pores. The experimental results confirmed this supposition. Indeed, for both the parent and the modified catalysts, the methyl mercaptan conversion was about 60 % (Fig. S11). As shown earlier by Huguet et al. [25], this value corresponds to the thermodynamic equilibrium at  $400 \pm 25 \text{ }^\circ\text{C}$ .

In contrast, the toluene conversion was highly dependent on the catalyst. As shown in Fig. 4, the deposition of a silica layer on the parent zeolite led to a decrease in the toluene conversion.

The initial conversion of toluene gradually decreased from 27 % for H-ZSM-5 to 15 % for the 12 % $\text{SiO}_2/\text{H-ZSM-5}$  catalyst. While over H-ZSM-5 and 4 % $\text{SiO}_2/\text{H-ZSM-5}$  the toluene conversion remained nearly constant during 400 min on stream, it slowly decreased during the reaction run for other two catalysts.

The data plotted in Fig. 5 show a very good relationship between the initial toluene conversion and the amount of Bronsted acid sites measured by pyridine adsorption (see also Table 1). These experimental results correspond to a turnover frequency of  $39 \text{ h}^{-1}$  (mol of converted toluene/mol of Bronsted acid sites  $\times$  h).

Under the reaction conditions used in the present study, the hydrocarbons formed during the process were almost entirely aromatics, with xylenes and trimethylbenzenes being the main molecules. Only traces of low aliphatic hydrocarbons were identified among the products (Fig. S12a and S12b). Fig. 6 shows the ratios between the aromatic hydrocarbons formed at the beginning (20 min on stream) and the end of the catalytic run (400 min on stream) over the parent and the modified zeolite.

The ratio gradually increases from 68:32 (for H-ZSM-5) to 95:5 (for 12 % $\text{SiO}_2/\text{H-ZSM-5}$ ), suggesting that the trimethylbenzenes are essentially formed on the external surface of the catalysts. As shown in Fig. 6, these compositions did not change during the 400 min of reaction.

The most important result of the present study concerns the distribution of xylenes. As shown in Fig. 7 and Table 6, an obvious increase of

**Table 5**

Rate constants (k) at different temperatures.

Temperature, $^\circ\text{C}$	375	400	425
k ( $\text{h}^{-1}$ )	1.6	2.5	4.2

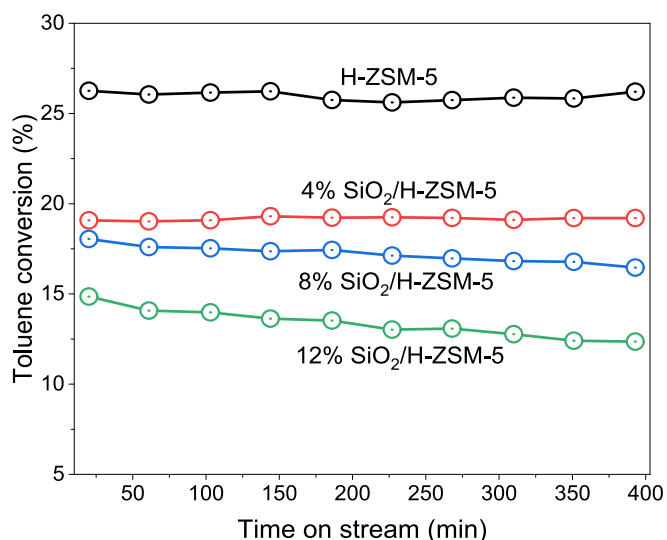


**Fig. 4.** Toluene conversion as a function of TOS; Conditions:  $m_{\text{cat}} = 30 \text{ mg}$ ,  $T = 375 \text{ }^\circ\text{C}$ , flow rate =  $30 \text{ mL min}^{-1}$ , toluene/ $\text{CH}_3\text{SH} = 1/1$ ,  $\text{WHSV} = 9.4 \text{ g}_{\text{toluene}+\text{CH}_3\text{SH}} \text{ g}_{\text{cat}}^{-1} \text{ h}^{-1}$ .

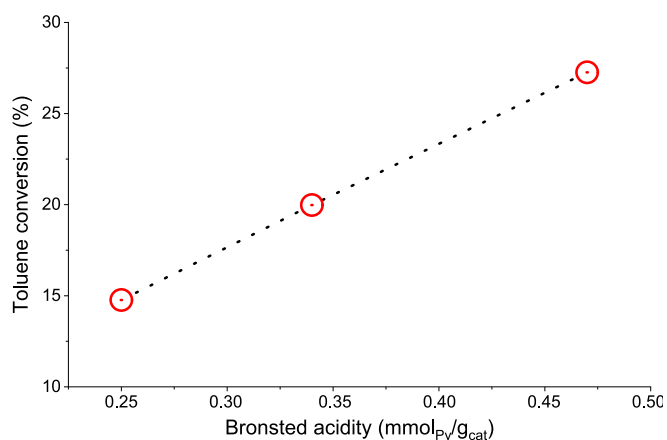


**Fig. 5.** Toluene conversion vs. Bronsted acidity. Conditions  $m_{\text{cat}} = 30 \text{ mg}$ ,  $T = 375 \text{ }^\circ\text{C}$ , flow rate =  $30 \text{ mL min}^{-1}$ , toluene/ $\text{CH}_3\text{SH} = 1/1$ ,  $\text{WHSV} = 9.4 \text{ g}_{\text{toluene}+\text{CH}_3\text{SH}} \text{ g}_{\text{cat}}^{-1} \text{ h}^{-1}$ , TOS = 20 min.

the *para*-selectivity was engendered by modifying the H-ZSM-5 zeolite with silica. The *para*-selectivity exhibited by the parent zeolite is 37 % and reached the remarkable value of 98 % in the presence of the 12 %  $\text{SiO}_2/\text{H-ZSM-5}$  catalyst.

Fig. 8 compares the *para*-selectivity of different catalysts with that of thermodynamic equilibrium (i.e. 25 % *para*-, 50 % *meta*- and 25 % *ortho*-xylene). Note that for each catalyst, the xylene distributions did not change during the 400 min on stream. In terms of *para*-selectivity, the results obtained in this study are comparable to the best results obtained in the alkylation of toluene with methanol, in the presence of modified H-ZSM-5 catalysts [12,17].

The yields in alkylation, xylenes and *para*-xylene are given in Fig. 9. These results show the very favorable effect of the zeolite modification on the catalyst performances, in particular on the *para*-selectivity.

Based on these results, it should be mentioned that the *para*-xylene yield obtained over 12 % $\text{SiO}_2/\text{H-ZSM-5}$  is twice than that obtained with unmodified zeolite.

### 3.2.4. Toluene alkylation by methyl mercaptan over 12 % $\text{SiO}_2/\text{ZSM-5}$ catalyst

In order to gather more information about the behavior of the 12 %

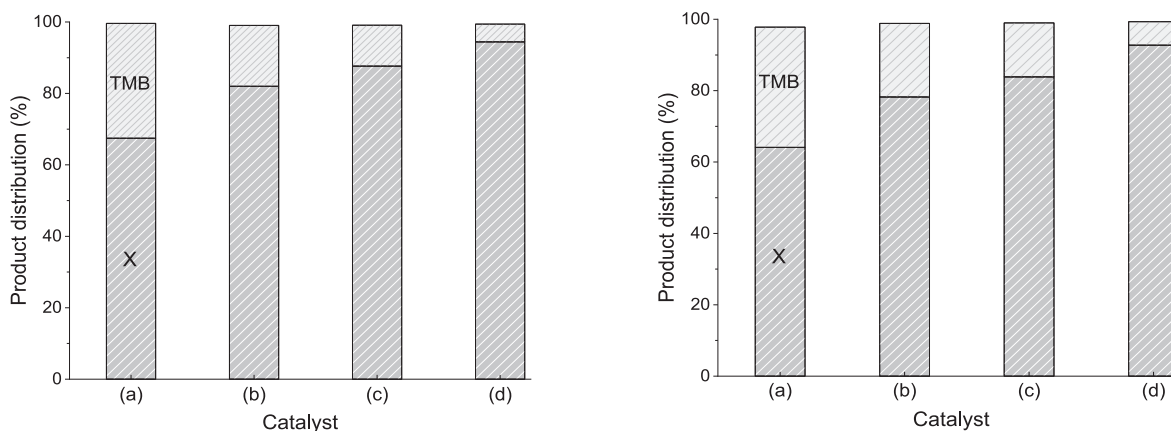


**Fig. 6.** Distribution of xylenes (X) and trimethylbenzenes (TMB) 20 min on stream (left) and 400 min on stream (right). (a) H-ZSM-5; (b) 4 %SiO<sub>2</sub>/H-ZSM-5; (c) 8 % SiO<sub>2</sub>/H-ZSM-5; (d) 12 %SiO<sub>2</sub>/H-ZSM-5. Conditions:  $m_{\text{cat}} = 30 \text{ mg}$ ,  $T = 375 \text{ }^\circ\text{C}$ , flow rate =  $30 \text{ mL min}^{-1}$ , toluene/CH<sub>3</sub>SH = 1/1, WHSV =  $9.4 \text{ g}_{\text{toluene}+\text{CH}_3\text{SH}} \text{ g}_{\text{cat}}^{-1} \text{ h}^{-1}$ , TOS = 20 min.

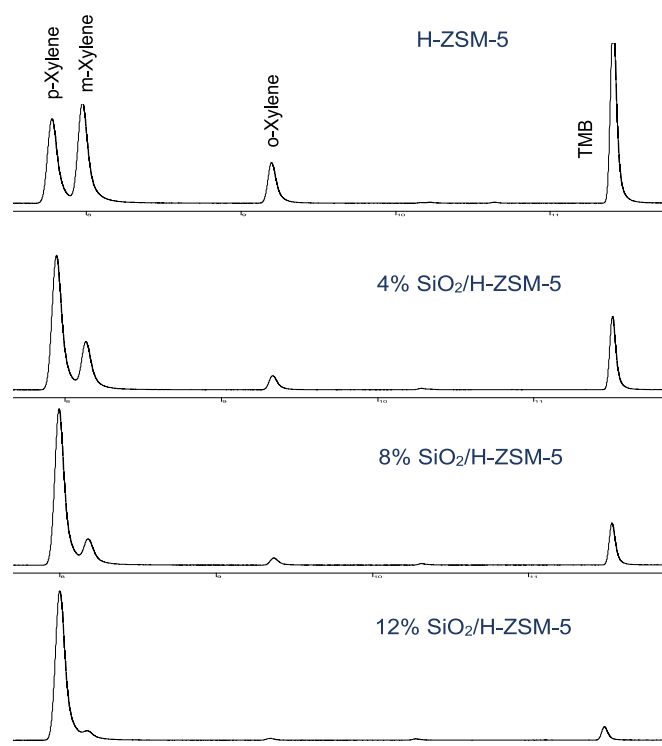


**Fig. 7.** GC-FID chromatograms of the aromatic hydrocarbons in the toluene alkylation carried out at  $375 \text{ }^\circ\text{C}$ . TOS = 20 min.

**Table 6**

Xylene distribution (%) in the toluene alkylation performed at  $375 \text{ }^\circ\text{C}$ . TOS = 20 min.

Catalyst	<i>para</i> -xylene	<i>meta</i> -xylene	<i>ortho</i> -xylene
H-ZSM-5	37	47	16
4 %SiO <sub>2</sub> /H-ZSM-5	68	26	6
8 %SiO <sub>2</sub> /H-ZSM-5	82	15	3
12 %SiO <sub>2</sub> /H-ZSM-5	98	1.5	0.5

SiO<sub>2</sub>/H-ZSM-5 catalyst, we examined the reaction between toluene and methyl mercaptan under diverse reaction conditions. To explore the effect of the temperature, the reaction was carried out at 375, 425 and 475 °C, using 30 mg of catalyst and a WHSV of  $9.4 \text{ g}_{\text{toluene}+\text{CH}_3\text{SH}} \text{ g}_{\text{cat}}^{-1} \text{ h}^{-1}$ .

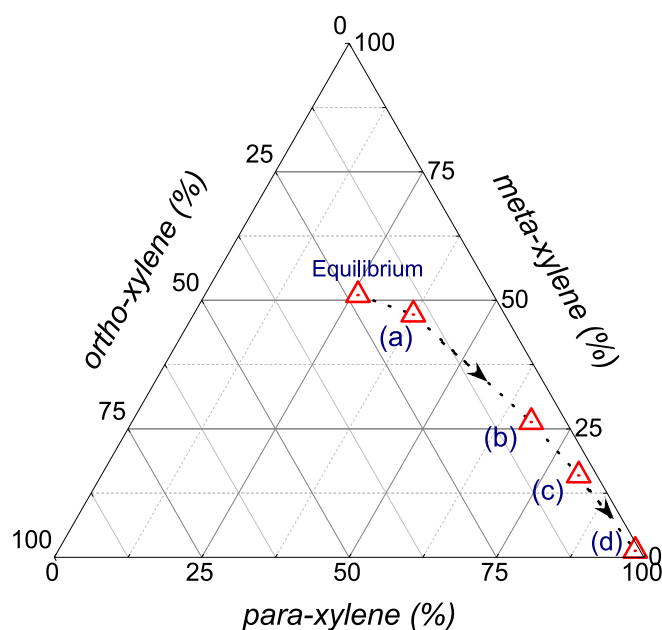


**Fig. 8.** Xylene isomers distribution in the alkylation process over different catalysts and at the thermodynamic equilibrium. (a) H-ZSM-5; (b) 4 %SiO<sub>2</sub>/H-ZSM-5; (c) 8 %SiO<sub>2</sub>/H-ZSM-5; (d) 12 %SiO<sub>2</sub>/H-ZSM-5. Experimental conditions: TOS = 20 min,  $m_{\text{cat}} = 30 \text{ mg}$ ,  $T = 375 \text{ }^\circ\text{C}$ , flow rate =  $30 \text{ mL min}^{-1}$ , toluene/CH<sub>3</sub>SH = 1/1, WHSV =  $9.4 \text{ g}_{\text{toluene}+\text{CH}_3\text{SH}} \text{ g}_{\text{cat}}^{-1} \text{ h}^{-1}$ , TOS = 20 min.

**Fig. 10** compares the profiles of the toluene conversion obtained at different temperatures. The initial conversion varied from 15 % at  $375 \text{ }^\circ\text{C}$ , to 41 % at  $475 \text{ }^\circ\text{C}$ . At 425 and  $475 \text{ }^\circ\text{C}$ , the loss in the activity over TOS was noticeable.

The initial methyl mercaptan conversion was about 60 % for each temperature. At  $375 \text{ }^\circ\text{C}$ , it did not vary during 400 min on stream. In contrast, it gradually and markedly decreased at 425 and  $475 \text{ }^\circ\text{C}$ , respectively (**Fig. S13**).

The initial C-containing products formed at  $375 \text{ }^\circ\text{C}$ , included xylenes, trimethylbenzenes, dimethyl sulfide and light hydrocarbons (**Fig. S14**). At  $425 \text{ }^\circ\text{C}$  and  $475 \text{ }^\circ\text{C}$  the initial amount of both aromatic and light hydrocarbons significantly increased to the detriment of dimethyl sulfide. Additionally, it should be underlining the substantial effect of the temperature on the *para*-selectivity, which decreased from 98 % at  $375 \text{ }^\circ\text{C}$  to 77 % at  $425 \text{ }^\circ\text{C}$  and 75 % at  $475 \text{ }^\circ\text{C}$ . Note, however, the weak effect of the temperature on the ratio between xylenes and TMBs. Due to

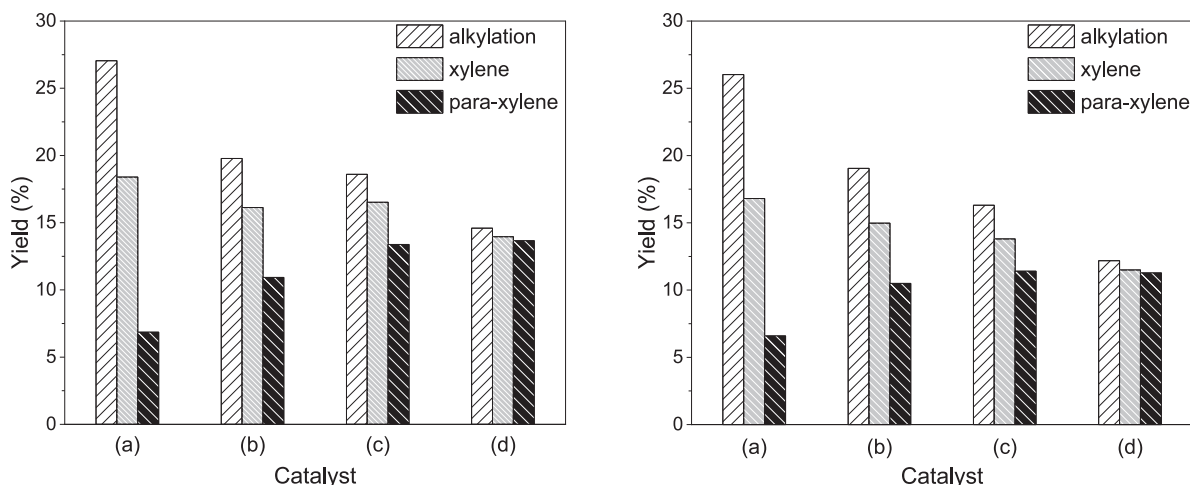


**Fig. 9.** Alkylation, xylene and *para*-xylene yields at 20 min on stream (left) and 400 min on stream (right); (a) H-ZSM-5; (b) 4 %SiO<sub>2</sub>/H-ZSM-5; (c) 8 %SiO<sub>2</sub>/H-ZSM-5; (d) 12 %SiO<sub>2</sub>/H-ZSM-5; yield = toluene conversion x selectivity in alkylation, xylenes or *para*-xylene. Conditions:  $m_{cat} = 30$  mg,  $T = 375$  °C, flow rate = 30 mL  $min^{-1}$ , toluene/CH<sub>3</sub>SH = 1/1,  $WHSV = 9.4$   $g_{toluene+CH_3SH} g_{cat}^{-1} h^{-1}$ .

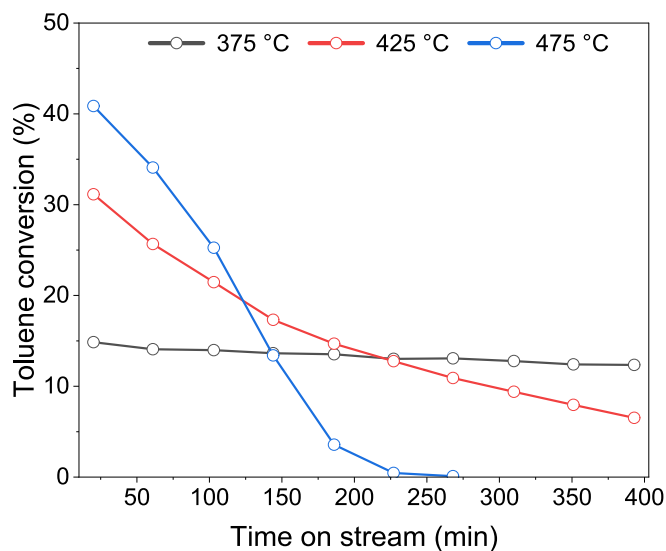


**Fig. 10.** Toluene conversion as a function of TOS and temperature over 12 % SiO<sub>2</sub>/H-ZSM-5. Conditions: 30 mg of catalyst,  $WHSV$  of 9.4  $g_{toluene+CH_3SH} g_{cat}^{-1} h^{-1}$ , toluene/CH<sub>3</sub>SH = 1/1.

the catalyst deactivation at 425 °C and 475 °C, the amount of the methylating compounds strongly diminished at 180 min on stream (Fig. S15).

In short, the experimental results suggest that in terms of both *para*-xylene yield and catalyst stability against deactivation, 375 °C is the most favorable temperature for our process.

As seen before, the 12 %SiO<sub>2</sub>/H-ZSM-5 catalyst underwent deactivation, especially at high reaction temperature. For this type of catalyst, the deactivation is typically due to the formation of bulky species (usually called “coke”) that lead to progressive pore blockage and/or coverage of the acid sites.

We examined the coke confined in the spent catalysts by TGA-MS, using the procedure described in the experimental section. The MS signals of CO<sub>2</sub> ( $m/z = 44$ ) and SO<sub>2</sub> ( $m/z = 64$ ) for the 12 %SiO<sub>2</sub>/H-ZSM-5 catalyst, after the tests carried out at three temperatures, are plotted in Fig. 11 Fig. S16. Note that the CO<sub>2</sub> and SO<sub>2</sub> MS signals come from the combustion of C- and S-containing species, respectively. According to TGA-MS results, the quantities of the heavy species retained on the spent catalysts seem comparable.

However, the nature of these species is different, depending on the reaction temperature. Thus, the main burning features (CO<sub>2</sub> peaks) displayed by the TGA-MS profiles are centered at about 575 °C, 600 °C and 610 °C for the catalytic test performed at 375 °C, 425 °C and 475 °C, respectively. On the other hand, in the TGA-MS profiles recorded for the catalyst used at 375 and 425 °C, no MS SO<sub>2</sub> peak was observed. In contrast, for the catalyst used at 475 °C, a small SO<sub>2</sub> MS peak appeared between 450 and 500 °C. This peak can be related to the combustion of heavy S-containing molecules, e.g. polysulfides located in the catalyst matrix. Note that the formation of such S-compounds from CH<sub>3</sub>SH has been previously reported by Yu et al. over SSZ-13 zeolite [26].

The absence of the SO<sub>2</sub> peak in the TGA-MS profiles at 375 and 425 °C proves that no amount of sulfur was imprisoned in the used catalyst. Consequently, it is reasonable to state that at these temperatures only the hydrocarbons, in particular the aromatics, were involved in the formation of the coke deposits. This result agrees with the so called “step-wise” mechanism described in Scheme 2 [27], which shows that during the toluene methylation, sulfur leaves the process early as H<sub>2</sub>S. Additionally, this proves that CH<sub>3</sub>SH is entirely involved in toluene alkylation and not in reactions leading to the formation of bulky S-containing molecules.

Next, we studied the effect of the spatial velocity (WHSV) on the alkylation process. Several tests were carried out by modifying the quantity of the catalyst in the reactor (Table 7).

The methyl mercaptan conversion was about 60 % in all tests. In contrast, the toluene conversion varied from 15 % (at  $WHSV = 9.4$ ) to 35 % (at  $WHSV = 1.9$ ) (Table 7). By analogy with the model used above, we treated the present results considering a first-order kinetic for toluene and zero-order for methyl mercaptan. We obtained a rate constant of 0.66  $h^{-1}$ .

The main C-containing molecules formed included xylenes, trimethylbenzenes, dimethyl sulfide and light hydrocarbons (Fig. S17). The amount of trimethylbenzenes slowly increased when the space velocity decreased, but the xylenes remain the dominant reaction products (> 90 %). Likewise, the amount of the light aliphatic hydrocarbons (especially ethylene) increased when the space velocity decreased.

The effect of the space velocity on the xylene isomers was also notable (Fig. 12). Thus, the *para*-selectivity decreased from 98 % (at  $WHSV = 9.4$ ) to 76 % (at  $WHSV = 1.9$ ). Fig. 13 also shows that the *para*-selectivity decreased when the toluene conversion increased.

To explain these results, we could consider the data previously reported for the alkylation of toluene with methanol. For example, it was shown that during the toluene methylation, the *para*-selectivity was mainly determined by the rates of two successive reactions, i.e., toluene



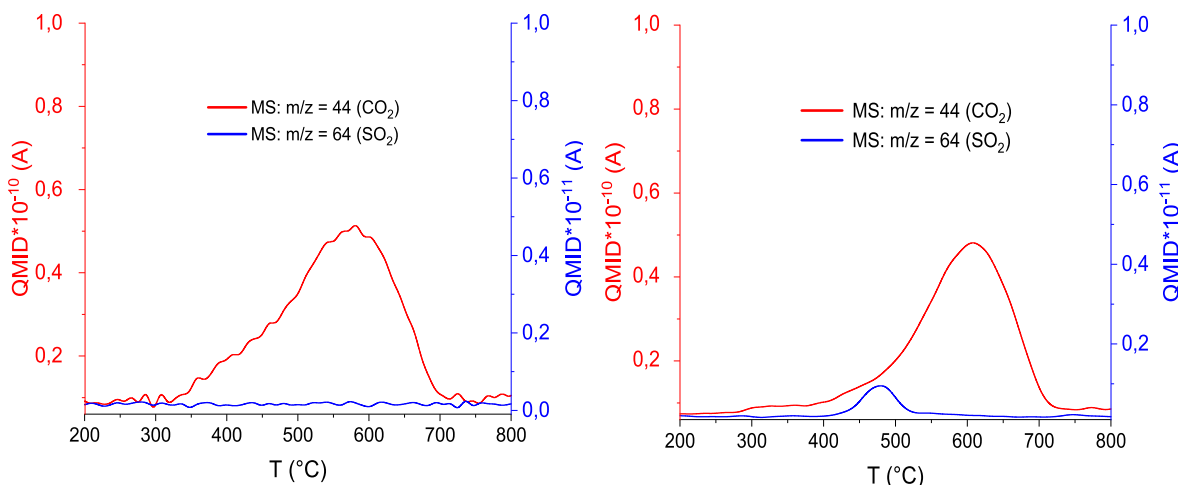
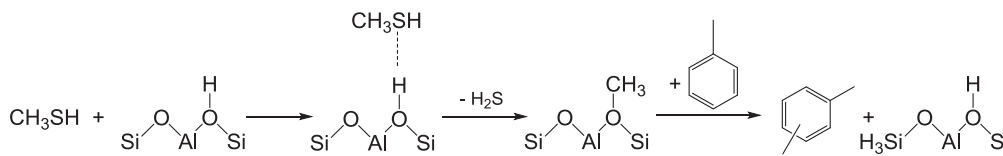


**Fig. 11.** MS signals of CO<sub>2</sub> (red,  $m/z = 44$ ) and SO<sub>2</sub> (blue,  $m/z = 64$ ) of the spent 12 %SiO<sub>2</sub>/H-ZSM-5 catalyst, after the catalytic tests carried out at 375 °C (left) and 475 °C (right). (For interpretation of the references to colour in this figure legend, the reader is referred to the web version of this article.)



**Scheme 2.** “Step-wise” mechanism for methylation of toluene by methyl mercaptan [according to ref. 27].

**Table 7**  
Initial toluene conversions at WHSV.<sup>a</sup>

WHSV ( $\text{g}_{\text{toluene}+\text{CH}_3\text{SH}} \text{g}_{\text{cat}}^{-1} \text{h}^{-1}$ )	$m_{\text{catalyst}}$ (mg)	Toluene conversion (%)
9.4	30	15
4.7	60	24
2.8	100	31
1.9	150	35

<sup>a</sup> Catalyst 12 %SiO<sub>2</sub>/H-ZSM-5, T = 375 °C.

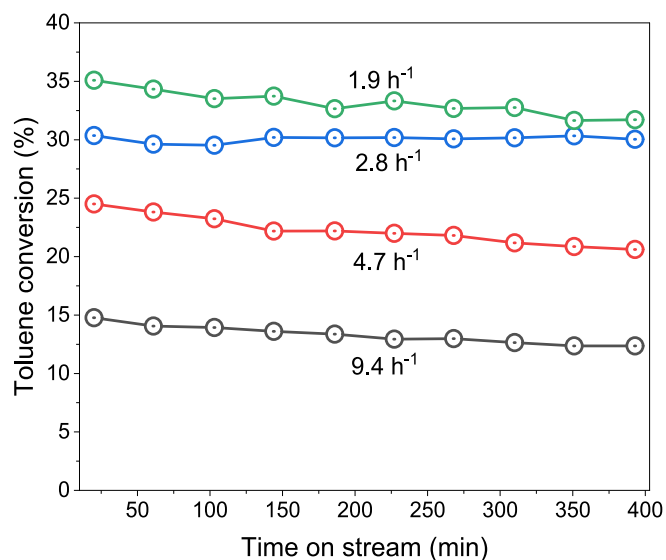


**Fig. 12.** Toluene conversion over 12 %SiO<sub>2</sub>/H-ZSM-5 as a function of TOS and WHSV; conditions:  $m_{\text{cat}} = 30$  mg, T = 375 °C, flow rate = 30 mL min<sup>-1</sup>, toluene/CH<sub>3</sub>SH = 1/1.

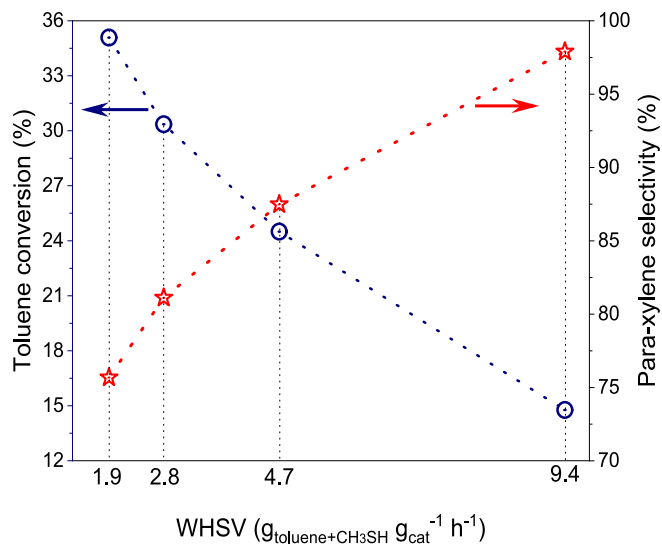


**Fig. 13.** Toluene conversion and *para*-selectivity vs. WHSV over 12 %SiO<sub>2</sub>/H-ZSM-5; conditions:  $m_{\text{cat}} = 30$  mg, T = 375 °C, flow rate = 30 mL min<sup>-1</sup>, toluene/CH<sub>3</sub>SH = 1/1.

methylation and the xylenes isomerization [28]. In our study, over 12 % SiO<sub>2</sub>/H-ZSM-5, at WHSV = 9.4  $\text{g}_{\text{toluene}+\text{CH}_3\text{SH}} \text{g}_{\text{cat}}^{-1} \text{h}^{-1}$  and 375 °C, the *para*-xylene was the major isomer. This is mainly due to the silylation, which strongly diminished the xylene isomerization over the external surface. On the other hand, it is known that the *para*-isomer is the primary xylene formed in the toluene alkylation by methanol [29]. To prevent the already formed *para*-xylene from coming into repeated contact with the acid sites inside the pores and thus limit its isomerization, it is necessary to reduce the contact time. In this context, it is important to mention the study published by Breen et al. [30]. By operating at a very short contact time (i.e. 0.17 s), over MgO-ZSM-5

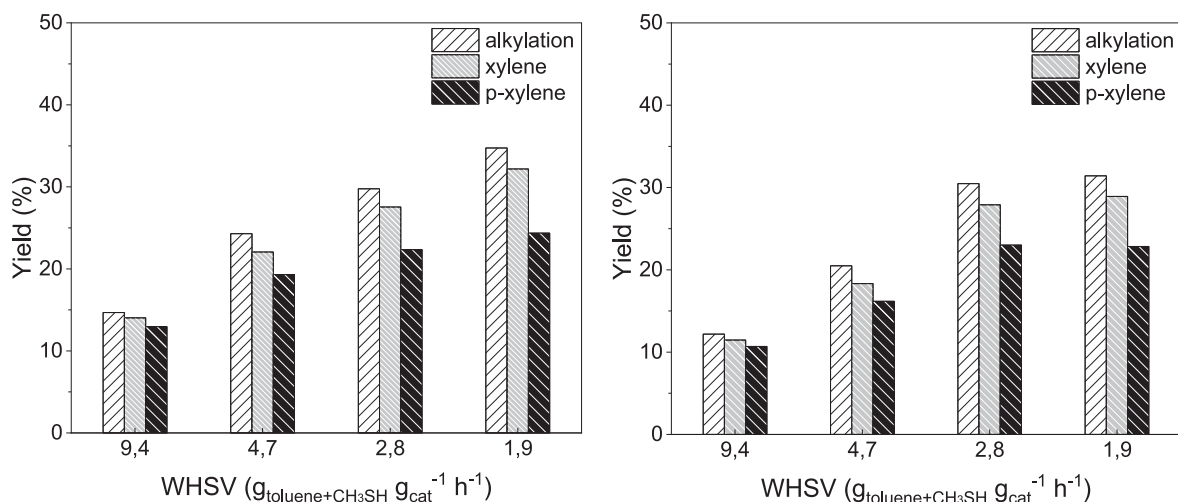


Fig. 14. Alkylation, xylene and *para*-xylene yields as a function of WHSV at 20 min on stream (left) and 400 min on stream (right). Toluene alkylation by methyl mercaptan over 12 %SiO<sub>2</sub>/H-ZSM-5. Conditions: m<sub>cat</sub> = 30 mg, T = 375 °C, flow rate = 30 mL min<sup>-1</sup>, toluene/CH<sub>3</sub>SH = 1/1.

catalyst, they showed that the *para*-selectivity was closed to 100 %.

Fig. 14 shows the effect of the spatial velocity on the yield in alkylation, in xylenes and in *para*-xylene. As we can observe, in terms of yields, the decrease of the space velocity (similar to the increase of the contact time) is very advantageous.

#### 4. Conclusions

This study showed that the modification of the H-ZSM-5 zeolite by external surface silylation is a very effective method for achieving high *para*-selective methylation of toluene by methyl mercaptan. At 375 °C and WHSV = 9.4 g<sub>toluene+CH<sub>3</sub>SH</sub> g<sub>cat</sub><sup>-1</sup> h<sup>-1</sup>, a selectivity close to 100 % was obtained with the 12 %SiO<sub>2</sub>/H-ZSM-5 catalyst. Additionally, under these conditions, this catalyst showed high stability against coke deactivation. Under more severe reaction conditions, i.e. higher temperature and lower WSHV, the yields of xylenes and *para*-xylene increased, but the catalyst deactivation over TOS was very pronounced.

It is important to note that some behavior presented in this study, such as the alkylation efficiency of both methyl mercaptan and toluene (higher than 98 %), as well as the selectivity to *para*-xylene, were superior to those reported in the literature for the toluene alkylation with methanol in the presence of ZSM-5 based-catalysts, under comparable process parameters.

#### CRedit authorship contribution statement

**Abdelilah Bayout:** Writing – original draft, Formal analysis, Data curation. **Claudia Cammarano:** Validation, Supervision, Conceptualization. **Izabel Medeiros Costa:** Validation, Supervision, Resources, Conceptualization. **Gleb Veryasov:** Validation, Supervision, Resources, Conceptualization. **Alexander Sachse:** Writing – review & editing, Writing – original draft, Data curation. **Vasile Hulea:** Writing – review & editing, Writing – original draft, Validation, Supervision, Project administration, Methodology, Conceptualization.

#### Declaration of competing interest

The authors declare that they have no known competing financial interests or personal relationships that could have appeared to influence the work reported in this paper.

#### Acknowledgements

This work was supported by TotalEnergies One Tech, Belgium.

AS acknowledges financial support from the European Union (ERDF), “Région Nouvelle Aquitaine” and to the French government program “Investissements d’Avenir” (EUR INTREE,

reference ANR-18-EURE-0010). Amine Geneste (PAC-ICGM) is thanked for the TGA-MS measurements. Olinda Gimello (ICGM), Johann Bale (ICGM) and Jean-Dominique Comparot (IC2MP) are thanked for their technical assistance throughout this research. We thank Dr. Anne Galarneau (ICGM) for her helpful assistance in the textural characterization of the catalysts.

#### Data availability

No data was used for the research described in the article.

#### References

- [1] A. Bayout, C. Cammarano, I.M. Costa, G. Veryasov, V. Hulea, Friedel-Crafts alkylation of toluene by methyl mercaptan - Effect of topology and acidity of zeolite catalysts, *ACS Catal.* 14 (2024) 3867–3877.
- [2] Source : BlueWeave Consulting, 2022. Available at : <https://www.blueweaveconsulting.com/report/global-paraxylene-market>.
- [3] L. Kumar, S. Asthana, B.L. Newalkar, K.K. Pant, Selective toluene methylation to p-xylene: current status & future perspective, *Catal. Rev.* (2022) 1–43.
- [4] D. Fraenkel, M. Levy, Comparative study of shape-selective toluene alkylation over HZSM-5, *J. Catal.* 118 (1989) 10–21.
- [5] J. Zhou, Z. Liu, Y. Wang, D. Kong, Z. Xie, Shape selective catalysis in methylation of toluene : Development, challenges ad catalysis, *Front. Chem. Sci. Eng.* 12 (2018) 103–112.
- [6] X. Huang, R. Wang, X. Pan, C. Wang, M. Fan, Y. Zhu, Y. Wang, J. Peng, Catalyst design strategies towards highly shape-selective HZSM-5 for *para*-xylene through toluene alkylation, *Green, Energy Environ.* 5 (2020) 385–393.
- [7] N. Chakinala, A.G. Chakinala, Process design strategies to produce p-xylene via toluene methylation: A review, *Ind. Eng. Chem. Res.* 60 (2021) 5331–5351.
- [8] L.B. Young, S.A. Butter, W.W. Kaeding, Shape selective reactions with zeolite catalysts : III. Selectivity in xylene isomerization, toluene-methanol alkylation, and toluene disproportionation over ZSM-5 zeolite catalysts, *J. Catal.* 76 (1982) 418–432.
- [9] G. Mirth, J. Cejka, J.A. Lercher, Transport and isomerization of xylenes over HZSM-5 zeolites, *J. Catal.* 139 (1993) 24–33.
- [10] Y. Bhat, J. Das, K. Rao, A. Halgeri, Inactivation of external surface of ZSM-5: zeolite morphology, crystal size, and catalytic activity, *J. Catal.* 159 (1996) 368–374.
- [11] C. Wang, L. Zhang, X. Huang, Y. Zhu, G. Li, Q. Gu, J. Chen, L. Ma, X. Li, Q. He, J. Xu, Q. Sun, C. Song, M. Peng, J. Sun, D. Ma, Maximizing sinusoidal channels of HZSM-5 for high shape-selectivity to p-xylene, *Nature Commun.* 10 (2019) 4348.
- [12] J. Cejka, N. Zilkova, B. Widhterlova, G. Elder-Mirth, J.A. Lercher, Decisive role of transport rate of products for zeolite *para*-selectivity: Effect of coke deposition and

- external surface silylation on activity and selectivity of HZSM-5 in alkylation of toluene, *Zeolites* 17 (1996) 265–271.
- [13] H.P. Röger, M. Krämer, K.P. Möler, C.T. O'Connor, Effects of in-situ chemical vapour deposition using tetraethoxysilane on the catalytic and sorption properties of ZSM-5, *Microporous Mesoporous Mater.* 21 (1998) 607–614.
- [14] J.H. Ahn, R. Kolvenbach, S.S. Al-Khattaf, A. Jentys, J.A. Lercher, Enhancing shape selectivity without loss of activity – novel mesostructured ZSM5 catalysts for methylation of toluene to p-xylene, *Chem Commun.* 49 (2013) 10584–10586.
- [15] W. Kaeding, C. Chu, L. Young, B. Weinstein, S. Butter, Selective alkylation of toluene with methanol to produce para-xylene, *J. Catal.* 67 (1981) 159–174.
- [16] N. Chen, W. Kaeding, F. Dwyer, Para-directed aromatic reactions over shape-selective molecular sieve zeolite catalysts, *J. Am. Chem. Soc.* 101 (1979) 6783–6784.
- [17] Y. Xie, B. Zhao, X. Long, Y. Tang, Dispersion of oxides on HZSM-5 and threshold effect on shape-selective methylation of toluene. In *Shape-Selective Catalysis: Chemicals Synthesis and Hydrocarbon Processing*; C. Song, J.M. Garcés, Y. Sugi Eds.; ACS Symposium Series, Vol. 738; American Chemical Society: Washington, DC, 1999; pp 188–200.
- [18] S. Zheng, H.R. Heydenrych, A. Jentys, J.A. Lercher, Influence of surface modification on the acid site distribution of ZSM-5, *J. Phys. Chem. B* 106 (2002) 9552–9558.
- [19] C. Zhang, X.W. Guo, C.S. Song, S.Q. Zhao, X.S. Wang, Effects of steam and TEOS modification on HZSM-5 zeolite for 2,6-dimethylnaphthalene synthesis by methylation of 2-methylnaphthalene with methanol, *Catal. Today* 149 (2010) 196–201.
- [20] N. Chakinala, A.G. Chakinala, Process design strategies to produce p-xylene via toluene methylation: A review, *Ind. Eng. Chem. Res.* 60 (2021) 5331–5351.
- [21] W. Alabi, L. Atanda, R. Jermy, S. Al-Khattaf, Kinetics of toluene alkylation with methanol catalyzed by pure and hybridized HZSM-5 catalysts, *Chem. Eng. J.* 195–196 (2012) 276–288.
- [22] J.L. Sotelo, M.A. Uguina, J.L. Valverde, D.P. Serrano, Kinetics of toluene alkylation with methanol over Mg-modified ZSM-5, *Ind. Eng. Chem. Res.* 32 (1993) 2548–2554.
- [23] J. Hill, A. Malek, A. Bhan, Kinetics and mechanism of benzene, toluene, and xylene methylation over H-MFI, *ACS Catal.* 3 (2013) 1992–2001.
- [24] H. Vinek, J.A. Lercher, Production and reactions of xylenes over H-ZSM5, *J. Mol. Catal.* 64 (1991) 23–39.
- [25] E. Huguet, B. Coq, R. Durand, C. Leroi, R. Cadours, V. Hulea, A highly efficient process for transforming methyl mercaptan into hydrocarbons and H<sub>2</sub>S on solid acid catalysts, *Appl. Catal. B, Environ.* 134–135 (2013) 344–348.
- [26] M. Yu, N. Tormene, A. Bolshakov, B. Mezari, A. Liutkova, N. Kosinov, E.J. M. Hensen, Selective methanethiol-to-olefins conversion over HSSZ-13 zeolite, *Chem. Commun.* 57 (2021) 3323–3326.
- [27] M. Reina, A. Martinez, C. Cammarano, C. Leroi, V. Hulea, T. Mineva, Conversion of methyl mercaptan to hydrocarbons over H-ZSM-5 zeolite : DFT/BOMD study, *ACS Omega* 2 (2017) 4647–4656.
- [28] J.H. Ahn, R. Kolvenbach, S.S. Al-Khattaf, J.A. Lercher, Methanol use in toluene methylation with medium and large pore zeolites, *ACS Catal.* 3 (2013) 817–825.
- [29] J.H. Ahn, R. Kolvenbach, O.Y. Gutierrez, S.S. Al-Khattaf, A. Jentys, J.A. Lercher, Tailoring p-xylene selectivity in toluene methylation on medium pore-size zeolites, *Microporous Mesoporous Mater.* 210 (2015) 52–59.
- [30] J. Breen, R. Burch, M. Kulkarni, P. Collier, S. Golunski, Enhanced para-xylene selectivity in the toluene alkylation reaction at ultralow contact time, *J. Am. Chem. Soc.* 127 (2005) 5021–5052.